

Article

Effect of Carrier Materials for Active Silver in Antibacterial Powder Coatings

Haiping Zhang ^{1,2}, Jixing Cui ¹, Jiayuan Yang ³, Hui Yan ¹, Xinping Zhu ^{4,5}, Yuanyuan Shao ⁶, Hui Zhang ^{3,*} and Jesse Zhu ⁴

¹ School of Chemical Engineering and Technology, Tianjin University, Tianjin 300072, China; hpzhang@tju.edu.cn (H.Z.); cuijixing@tju.edu.cn (J.C.); 2020207045@tju.edu.cn (H.Y.)

² Zhejiang Institute of Tianjin University, Shaoxing 312300, China

³ School of Chemical Engineering and Light Industry, Guangdong University of Technology, Guangzhou 510006, China; 2112206088@mail2.gdut.edu.cn

⁴ Department of Chemical and Biochemical Engineering, Western University, London, ON N6A 3K7, Canada; xzhu269@uwo.ca (X.Z.); jzhu@uwo.ca (J.Z.)

⁵ Wesdon River Powder Paint Scientific Research Co., Ltd., Foshan 528200, China

⁶ Nottingham Ningbo China Beacons of Excellence Research and Innovation Institute, The University of Nottingham Ningbo China, Ningbo 315100, China; yuanyuan.shao@nottingham.edu.cn

* Correspondence: hzhang1@uwo.ca

Abstract: Environmentally friendly powder coatings which have the advantages of being VOC-free, low-cost, and high-efficiency with a high recovery rate have been attracting increasing research attention. The introduction of antibacterial agents into the powder coatings endows them with a capacity to kill bacteria and viruses on the surface of objects; additionally, this enables them to inhibit the indirect transmission of pathogenic microorganisms. Silver, possessing broad-spectrum, strong, and stable antibacterial properties, is considered to be a promising antibacterial material for use in coating applications. Carrier materials for active silver play an important role in its activity and stability. However, there is a lack of systematic studies on the effects of different types of carriers in such coating systems, especially in green powder coating systems. In this paper, we investigated two types of carriers for active silver agents: zeolite, i.e., Linde type A (LTA) zeolite and Y-type zeolite; clay-based materials, i.e., montmorillonite and vermiculite. All the agents showed high antibacterial activity, with antibacterial rates of over 99% as compared to commercial agents. Among the four agents, the Ag-LTA zeolite antimicrobial agent showed a reduction rate of over 99.99%; additionally, it maintained a reduction rate of 99% after seven washing cycles. Thus, this agent was demonstrated to have the highest effectiveness and high durability; these features can be attributed to the high silver content and small particle size. The LTA zeolite also provides a protective effect for silver ions, protecting them from reduction, due to the restriction of elemental silver formation within the confined interior space of the α -cage structure. The Y-type zeolite antimicrobial agent exhibited a slightly lower antimicrobial performance due to its higher silicon-to-aluminum ratio and its lower cation exchange capacity. Comparatively, antimicrobial agents utilizing clay-based carriers have lower cation exchange capacity, resulting in poorer antimicrobial effectiveness than zeolite carriers. In addition, silver loaded on clay-based materials is prone to detach from the carrier and undergo a reduction reaction, making the coating yellowish in color. This study first provides information on the roles of different types of carriers in powder coating systems; then, this information guides the selection of carriers for active silver for the development of efficient antimicrobial agents and coatings.

Keywords: antimicrobial agent; powder coating; carrier; silver; zeolite; clay



Citation: Zhang, H.; Cui, J.; Yang, J.; Yan, H.; Zhu, X.; Shao, Y.; Zhang, H.; Zhu, J. Effect of Carrier Materials for Active Silver in Antibacterial Powder Coatings. *Coatings* **2024**, *14*, 297. <https://doi.org/10.3390/coatings14030297>

Academic Editors: Egemen Avcu, Yasemin Yildiran Avcu and Mert Guney

Received: 10 January 2024

Revised: 24 February 2024

Accepted: 27 February 2024

Published: 28 February 2024



Copyright: © 2024 by the authors. Licensee MDPI, Basel, Switzerland. This article is an open access article distributed under the terms and conditions of the Creative Commons Attribution (CC BY) license (<https://creativecommons.org/licenses/by/4.0/>).

1. Introduction

Biological contamination poses a continuous health risk, as surfaces often serve as a medium for bacteria and other microorganisms, enabling their rapid reproduction and

transmission. Microorganisms can survive on inanimate surfaces for hours, days, and weeks, or even longer. For instance, the COVID-19 coronavirus had a half-life of 18 h at a temperature of 21–24 °C and a relative humidity of 20% [1]. Disease transmission occurs significantly through surface contact between individuals, between animals and humans, and between animals themselves. Conventional protective and decorative coatings lack antibacterial properties, making these surfaces not only potential transmission vectors for pathogens but also susceptible to mold infestation [2]. This poses a significant challenge for coatings containing high levels of organic compounds. Therefore, antibacterial coatings which can kill the bacteria and viruses on the surfaces of objects are of great importance in preventing the indirect transmission of pathogenic microorganisms. Existing regular coatings mainly comprise solvent coatings, aqueous coatings, powder coatings, etc. Compared to solvent coatings, which cause the emission of VOCs, increasing research attention has been focusing on the production of environmentally friendly powder coatings which have the advantages of being VOC-free, low-cost, and high-efficiency, with a high recovery rate of 98% [3]. Powder coatings generally contain resin, a curing agent, a filler, pigment, and other additives. These gradients are mixed, extruded into chips, and ground into coating powders, which are then electrostatically sprayed onto the substrate and cured upon heating, forming a durable coating film. Due to the advantages of powder coatings, functional antimicrobial powder coatings have become an important research direction in the coating industry [4].

Antimicrobial powder coatings are fabricated by adding antimicrobial agents into coatings to realize a sterilization ability. In comparison with other antimicrobial heavy metals, silver is considered to be an exceptionally promising antibacterial material for use in coating systems because it offers numerous advantages, i.e., safety, broad-spectrum efficacy, long-lasting effects, and significant inhibition [5]. The WHO and US EPA have concluded that silver levels of 0.1 mg/L are tolerable in drinking water, and the EFSA (European Food Safety Agency) recommends thresholds of 0.05 mg/L in water and 0.05 mg/kg in food [6]. The concentration of silver which allows for antimicrobial activity can be as low as 10^{-4} mg/L; this is well below the threshold values, indicating the safety of applications involving silver [7–9]. It is generally believed that positively charged silver metal ions can effectively bind to the surface of bacterial cell membranes, facilitated by electrostatic attraction; subsequently, they penetrate the cell wall, causing it to rupture and leading to the release of cellular contents, ultimately resulting in bacterial death [10,11]. Silver ions are generally loaded onto carrier materials and then introduced to coating systems. Carrier materials should have some important parameters, including unique characteristics in cation exchange capacity and pore structure, as these aspects influence the function of the active components. It is widely reported that zeolite- and clay-based materials can serve as carriers for silver ions [12–14]. Zeolite carriers possess a framework of silicate with high adsorption and ion exchange capabilities, which permits them to act as inorganic reservoirs for silver ions [15–18]. N. Torkian et al. employed modified zeolite as a silver ion carrier to produce a Ag-ion-exchanged nanocomposite and successfully applied it in antibacterial applications [18]. Clay-like carriers have a layered silicate structure that can hold cations to maintain electrical neutrality and an abundant interlayer pore structure for the accommodation of silver ions or other cations [19–21]. In addition, they also have the advantages of natural abundance and cost effectiveness, a non-toxic nature, and chemical inertness [22]. In the study by W. Guo et al., silver was loaded into the interlayer space of montmorillonite, which endowed the PGA scaffold with sustained Ag⁺ release and long-lasting antibacterial properties [23].

These materials have been well reported as silver ion carriers, and most studies have generally adopted one or one-type carrier material; for example, Cerrillo et al. applied zeolite in the preparation of antimicrobial agents [12], and Malachová used montmorillonites as active ion carriers [24]. However, the effect of different types of carriers on silver antimicrobial activity and stability in coating systems, especially in powder coatings, is rarely studied. The curing of powder coatings requires high-temperature treatment, which

can reach a maximum of 200 °C [25]. Under this extreme-heat condition, silver ions are susceptible to reduction, forming yellow metallic silver particles, which leads to yellowing of the coating surface; this decreases the aesthetic appearance and also deactivates the active silver, decreasing the antimicrobial activity. Carrier materials can provide a protective effect for silver ions; the geometric properties and the binding affinity of carriers to silver may vary. To investigate their influence on silver activity and stability as well as the coating properties, two widely used zeolite materials (Linde type A and Y-type) and two clay-based materials (montmorillonite and vermiculite) were utilized to produce ion-exchange antimicrobial agents and their antimicrobial effectiveness in powder coatings was evaluated. The protection of carriers on Ag⁺ was also investigated via a color difference test, considering the tendency for Ag⁺ oxidation to occur under the high-temperature condition during powder coating production and curing.

2. Experimental Section

2.1. Materials

Linde type A (LTA) zeolite, which is a crystalline aluminosilicate material with a Si/Al ratio of around 1, was purchased from the PQ Corporation (Malvern, PA, USA), with a particle size of 2–3 µm; the Y-type zeolite was from Zibo Runxin Chemical Technology Co., Ltd. (Zibo, China), with a Si/Al ratio of 5 and a particle size of 4–5 µm. Montmorillonite (Model K10) was supplied by Clariant Chemical (China) Ltd. (Shanghai, China), with a whiteness of 40%–50% and a moisture content of 8%–12%; the vermiculite sample was from Hebei Jinghang Mineral Products Co., Ltd. (Shijiazhuang, China). Silver nitrate (purity > 99.9%) was from Aladdin Reagent (Shanghai) Co., Ltd. (Shanghai, China). All the chemicals were analytically pure. The commercial antibacterial agents Zeomic AJ10N/D and Zeomic AW10N/D were from Sinanen Zeomic Co., Ltd. (Nagoya City, Japan), and the Microkiller SRT-104 was from Japan's Ishizuka Glass Co., Ltd. (Iwakura-shi, Japan). The polyester coating used in this study was obtained from Guangdong Huajiang Powder Technology Co., Ltd. (Zhaoqing, China).

2.2. Preparation of Antibacterial Agents and Coatings

2.2.1. Preparation of Antibacterial Agents

The experiment compared the antibacterial effects of several carriers: LTA zeolite, Y-type zeolite, montmorillonite, and vermiculite. The vermiculite sample was first ground and sieved to obtain samples with a medium particle size of approximately 30 µm; these were then transferred to a 0.05 mol/L sodium nitrate solution and stirred continuously for 24 h to ensure that all impure ions in the vermiculite were converted into sodium ions. Measures of 5 g of LTA zeolite, Y-type zeolite, montmorillonite, and prepared vermiculite were added to 0.03 mol/L silver nitrate solution, respectively, and the pH of the suspensions was adjusted between 4 and 7 with nitric acid. The suspensions were stirred continuously at 25 °C for 5 h in the dark throughout the entire process. After that, they were centrifuged at a speed of 3500 rpm for 5 min and washed until no silver ion residues were detected. The solid samples were then dried at 50 °C and ground to obtain the antibacterial agents. The antibacterial agents were denoted as Ag-LTA, Ag-Y, Ag-M, and Ag-V for the carriers of LTA zeolite, Y-type zeolite, montmorillonite, and vermiculite, respectively.

2.2.2. Preparation of Antimicrobial Coatings

The preparation of polyester powder coatings involves pre-mixing, melt extrusion, and grinding. Initially, the resin, curing agent, and other additives were weighed and mixed in the setting proportions. The mixture was then placed in a pre-mixer for approximately 30 s to achieve a uniform dispersion. Subsequently, the pre-mixed material underwent further processing using a twin-screw extruder (SLJ-10, Yantai Donghui Powder Processing Equipment Co., Ltd., Yantai, China). The screw was set to rotate at 500 rpm, and the temperatures in regions 1, 2, and 3 of the extruder were set to 100 °C, 100 °C, and 110 °C, respectively. The hot extrudates were cooled, crushed into small chips, and added into an

air classifier mill (ACM-02, Yantai Donghui Powder Coating Processing Equipment Co., Ltd., Yantai, China) for grinding, classifying, and screening to obtain the final polyester coating powder.

The antimicrobial agents (2.0 wt.%) were fully mixed with the polyester powder coating. The antibacterial powder was sprayed onto the aluminum plate using a corona electrostatic spray gun (Surecoat, Nordson Corp., Westlake, OH, USA) with an operating voltage of 40 kV. All the panels were cured at 200 °C for 10 min in a convection oven (Wanrui Corp., Shanghai, China). The preparation process of antibacterial agents and coatings is shown in Figure S1.

2.3. Characterization of Antimicrobial Agents and Coatings

2.3.1. Characterization of Carrier and Antimicrobial Agents

The specific surface area, pore volume, and average pore diameter of four carriers were measured at 77 K using a specific surface area and porosity analyzer (ASAP2460, Micromeritics, Norcross, GA, USA). The specific surface area of the carriers was calculated using the Brunauer–Emmett–Teller (BET) method with linear region in the P/P_0 range of 0.10–0.30. The average pore diameter of zeolite-based carriers was calculated using the H-K method; that of clay-based carriers was estimated by the BJH method, based on the adsorption curves. The cation exchange capacity (CEC) of carriers was determined according to the method proposed by Kitsopoulos et al. [26]. The carriers were first saturated with NH_4^+ , which was subsequently converted to NH_3 . The exchange capacity was estimated from the amount of released NH_3 . The morphologies of carriers, antibacterial agents, and coatings were observed using scanning electron microscopy (S-4800, HITACHI, Tokyo, Japan). The distribution of silver in antibacterial agents was analyzed by energy-dispersive X-ray spectroscopy (EDS). The silver content was tested by inductively coupled plasma mass spectrometry (ICP-MS, Thermo iCAP-Q, <https://www.thermofisher.cn/cn/zh/home/industrial/mass-spectrometry/inductively-coupled-plasma-mass-spectrometry-icp-ms/single-quadrupole-inductively-coupled-plasma-mass-spectrometry-sq-icp-ms.html>, accessed on 26 February 2024). X-ray photoelectron spectroscopy was executed to assess the chemical state of Ag using a Thermo Fischer ESCALAB 250Xi (Waltham, MA, USA) equipped with an Al $K\alpha$ X-ray source.

The minimal inhibition concentration of antimicrobial agents with different carriers was tested. A measure of 0.5 mL of 10^6 CFU/mL *Escherichia coli* solution was taken and diluted in 5 mL LB liquid medium. Measures of 0.5 mL of deionized water and 0.5 mL of antibacterial agent suspension of different concentrations were added to the prepared medium solutions, respectively. The absorbance of the bacterial suspensions was measured at 600 nm every 2 h for 24 h using a UV–visible spectrophotometer (DR6000, 190–1100 nm, HACH, Ames, IA, USA).

The Kirby–Bauer test, also known as the disk-diffusion method, was used to evaluate the activity of antimicrobial agents. The procedure was performed as follows: A volume of 0.5 mL of a bacterial suspension with a concentration of 10^6 CFU/mL was added to the Mueller–Hinton (MH) culture medium and evenly spread using a sterile spreader. Filter paper discs with a diameter of 6 mm were cut and soaked in a suspension of 2 mg/mL antimicrobial agents. After drying, the filter paper discs containing the antimicrobial agent were placed on the surface of the MH agar. The plates were then incubated in a biochemical incubator (SPX-70BIII, Tianjin Taisite Instrument Co., LTD, Tianjin, China) at 37 °C for 24 h. The disk-diffusion test was also conducted directly with powder samples. The same amount of agent powder was pressed into pellets with a diameter of around 6 mm, and then put onto the MH agar to be incubated for 24 h. The diameter of the inhibition zone in both methods was measured accurately using a vernier caliper. The size of the inhibition zone indicates the antimicrobial effectiveness of the tested agent. All the tests were conducted three times, and the average was calculated.

2.3.2. Characterization of Antimicrobial Coatings

The thickness of the coating film was measured by a PosiTector 6000 thickness meter (DeFelsko Corporation, Ogdensburg, NY, USA). The impact resistance of the coating films was characterized by an impact tester according to GB/T 1732-2020 [27]. A steel weight of 1 kg was dropped from a height of 50 cm onto the coating film. If no crack was observed, it indicated that the coating can stand an impact of 490 N·cm and passed the test. The pencil scratch hardness test used constant pressure and special pencils (from 9H to 9B degrees) to scratch the finished film to determine the hardness of the film according to ASTM D3363-05-2011 [28]. The adhesion strength of coating samples was evaluated followed by GB/T 9286-1998 [29]. The coating was cross scratched and peeled by 3M tape. If no material was peeled off, then rate of coating was 0, suggesting excellent adhesive strength with the substrate.

The antibacterial tests of coating surface were conducted following ASTM E2180-07 [30]. The number of microorganisms was measured before and after inoculation. Each test was performed in triplicate, and the logarithmic mean value of the bacteria number was taken.

$$\text{Reduction rate (\%)} = \frac{X_0 - \bar{X}}{X_0} \times 100\% \quad (1)$$

where \bar{X} and X_0 stand for the logarithmic mean value of organisms after 6 h' incubation on the antibacterial coating and the control coating, respectively.

The durability of the coated surface was assessed by subjecting it to repeated cleaning with soap and water using the following procedure: The coating surface was wiped back and forth under a pressure of 20 kPa using a sponge (2 cm × 2 cm) soaked in soapy water a total of 60 times at room temperature. Subsequently, the surface was cleaned with 50 mL of water, marking the completion of one cycle. The antibacterial efficiency of the same coating surface was tested after each washing cycle according to ASTM 2180-07, using new active bacteria to determine the antimicrobial durability.

The color change of the coatings was determined using a colorimeter (WF32, Shanghai Jiabiao Co. Ltd., Shanghai, China). It is capable of measuring ΔE , ΔL , Δa , and Δb . ΔL represents the variation in brightness of the coating between black (0) and white (100), Δa indicates the change between red (+) and green (−), and Δb denotes the shift between yellow (+) and blue (−). The total color change can be calculated as follows:

$$\Delta E = \sqrt{\Delta L^2 + \Delta a^2 + \Delta b^2} \quad (2)$$

To test the release of silver ions on the coating surface, a leaching test was performed. The coating film was immersed to 0.9 wt % NaNO₃ solution (pH around 7) and the concentration of silver ions was tested after exposure for 6 h.

3. Results and Discussion

3.1. Analysis of Antibacterial Agents and Carriers

Table 1 presents the cation exchange capacity, specific surface area, pore volume, and average pore size of the four carriers. The table reveals that zeolite carriers possess a higher ion exchange capacity compared to clay-based carriers, attributed to their low silicon–aluminum ratio and higher aluminum content, which requires more cations for charge balance. There are a large number of exchangeable cations in the internal space. The LTA zeolite exhibits a lower Si/Al ratio than the Y-type zeolite, resulting in a higher exchange capacity. On the other hand, montmorillonite carriers only have exchangeable cations between their layers, which are limited in number.

In terms of surface area, zeolite carriers have a larger surface area than clay-based carriers. This is due to their refined and intricate structure, featuring more nanopores and a greater internal surface area, as well as smaller particle sizes. While there is not a noticeable difference in pore volume, zeolite carriers tend to have a slightly larger volume than

clay-based carriers. The most significant distinction lies in the average pore size. Zeolite sieve carriers possess significantly smaller pore sizes than clay-based materials, which is attributed to their structure. The pore channels of zeolite are typically the size of the minimum diameter of the α -cage, whereas the pore size of clay-based carriers corresponds to the interlayer domain distances, which are considerably larger than the α -cage diameter of zeolite.

Table 1. CEC, surface area, pore volume, and average pore size of several carrier samples.

Samples	CEC (meq/g)	Specific Surface Area (m ² /g)	Pore Volume (cm ³ /g)	Average Pore Diameter (nm)
LTA zeolite	5.21	557	0.57	0.39
Y-type zeolite	3.17	648	0.38	0.74
Montmorillonite	1.06	255	0.31	6.25
Vermiculite	0.76	194	0.30	6.20

Figure 1 shows the SEM images of four types of carriers, indicating the presence of layered structures on the surface morphologies of montmorillonite and vermiculite. Among them, the particles of montmorillonite are relatively small, ranging from approximately 20 to 30 μ m. A fine layered structure with a large number of mesopores and macropores on the surface can be seen. The layered structure of vermiculite has large voids, with single-layered stacking to form a thicker structure, making it a typical layered silicate. Vermiculite particles are larger and have a wide particle size distribution, with a medium particle size of approximately 70 μ m. Most particles do not produce thicker layers. Due to the large size of vermiculite particles, grinding was carried out to decrease the medium size to 30 μ m before ion exchange. Both Y-type and LTA Zeolite carriers exhibit regular geometric shapes of small squares with a particle size between 1 and 5 μ m. The particle size would have a large impact on their distribution on coatings and the final coating properties.

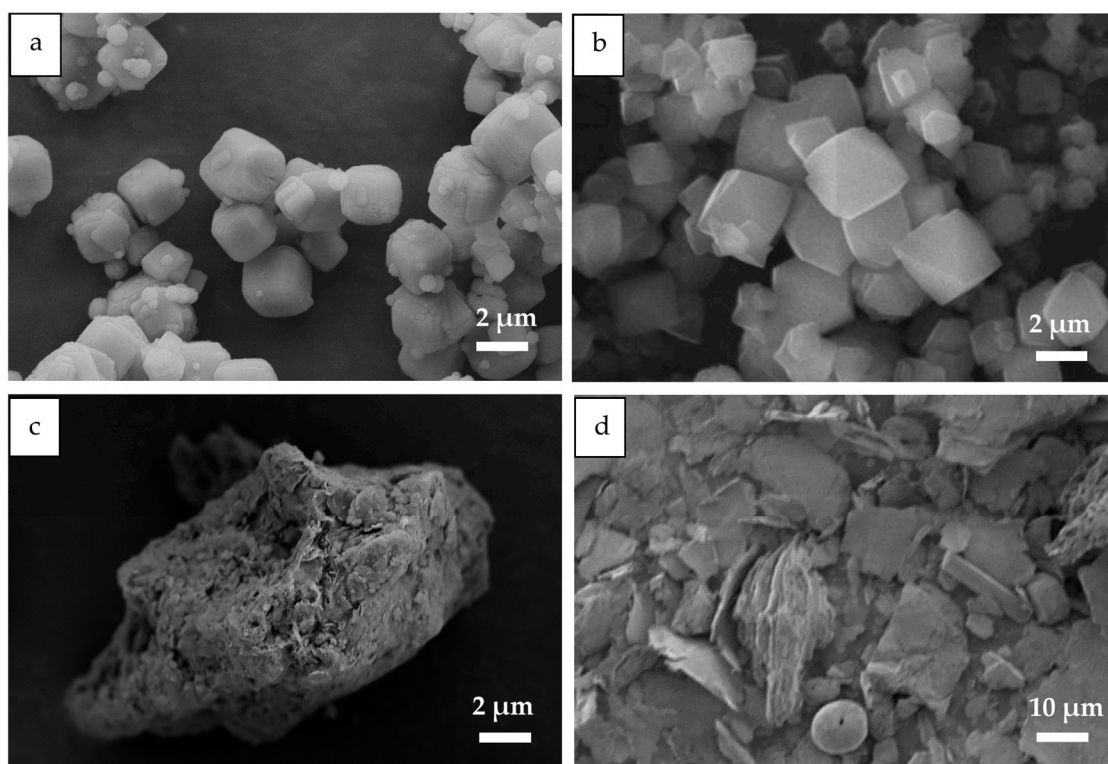


Figure 1. Scanning electron micrograph of four carriers: (a) LTA zeolite; (b) Y-type zeolite; (c) montmorillonite; (d) vermiculite.

The silver distribution and content were characterized by SEM-EDS mapping and ICP testing, as shown in Figure 2 and Table 2. The silver content in the antimicrobial agents is in the order of Ag-LTA > Ag-Y > Ag-M > Ag-V, which is consistent with the carriers' CEC results. As seen from the EDS mapping, silver is uniformly distributed on the carriers. The zeolite materials have better silver-accommodation ability compared to clay-based carriers.

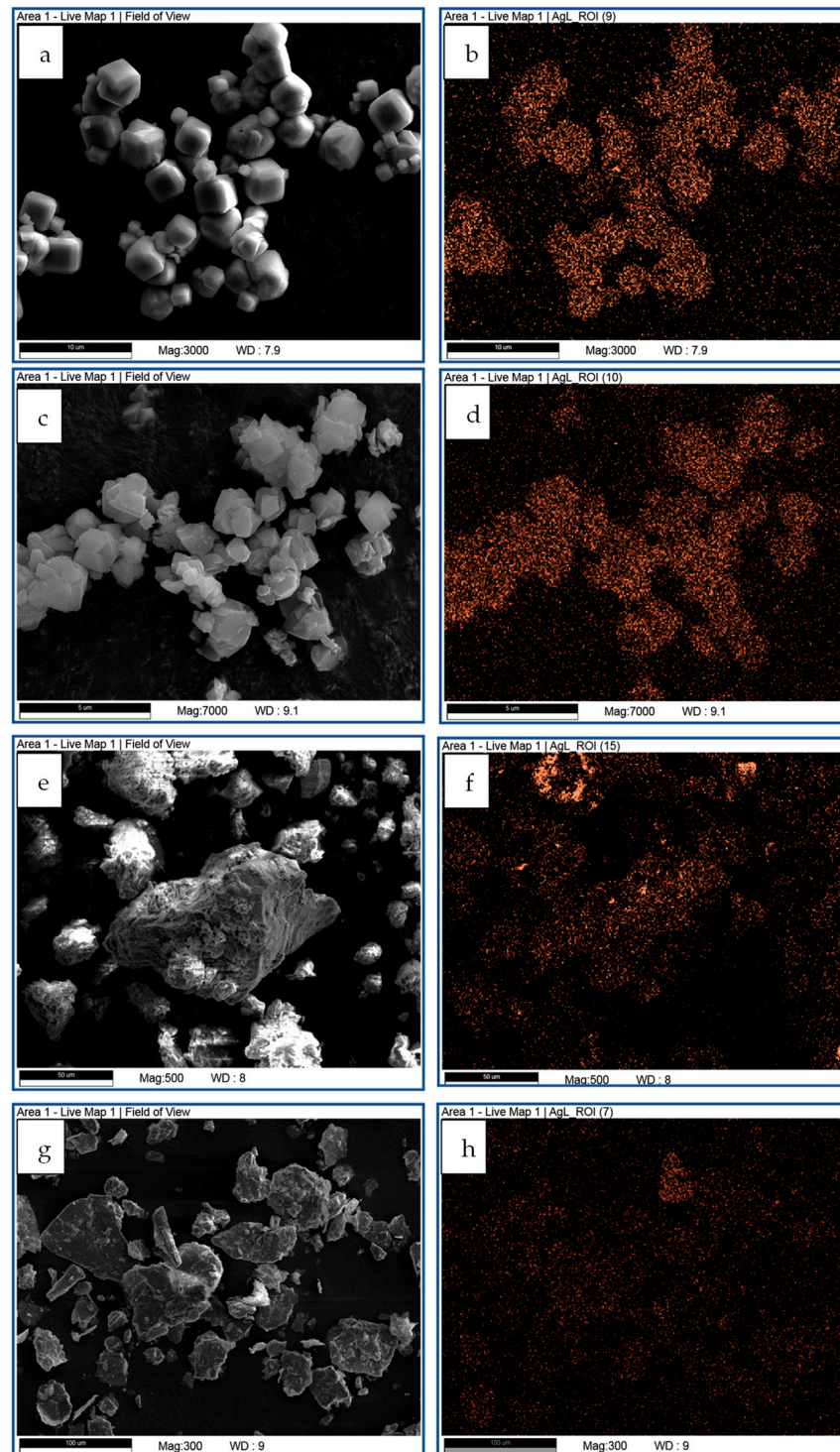


Figure 2. SEM images and EDS mapping of element Ag in antimicrobial agents: (a,b) Ag-LTA; (c,d) Ag-Y; (e,f) Ag-M; (g,h) Ag-V.

Table 2. Amounts of silver in different antimicrobial agents tested by ICP-MS.

Antibacterial Agents	Ag-LTA	Ag-Y	Ag-M	Ag-V
Ag (wt%)	11.4 ± 0.2	9.5 ± 0.4	3.9 ± 0.3	2.8 ± 0.2

3.2. Antibacterial Properties of Antibacterial Agents

To evaluate the antimicrobial efficacy of various antimicrobial agents, their minimum inhibitory concentrations (MICs) were determined. The antimicrobial agents were added to bacterial suspensions with initial concentrations of approximately 10^5 CFU/mL, and the absorbance was measured over time. This quantitative assessment method enables the rapid evaluation of antimicrobial activity.

Figure 3 clearly demonstrates that all tested antimicrobial agents had an impact on the growth kinetics of *E. coli* compared to the control group. As the concentration of the antimicrobial agent increased, the inhibitory effect on bacterial growth intensified. The Ag-LTA antimicrobial agent, for instance, achieved complete inhibition at a concentration of 150 µg/mL, while the corresponding concentrations for Ag-Y, Ag-M, and Ag-V were 250 µg/mL, 400 µg/mL, and 600 µg/mL, respectively (Table 3). It is worth noting that Ag-LTA exhibited the strongest antimicrobial activity against *E. coli*, requiring the lowest concentration among the tested agents to inhibit bacterial growth. Consequently, the addition of the Ag-LTA zeolite antimicrobial agent in practical applications would necessitate a smaller dosage, minimizing its impact on powder coating layers. As the antimicrobial agent concentrations increased from 0 to 70 µg/mL, the absorbance reductions within 24 h were 32.6 %, 16.5 %, 3.2 %, and 2.7 % for the respective antimicrobial agents. These results highlight the rapid antimicrobial rate and high effectiveness of the additives with the zeolite carrier; in contrast, clay-based materials exhibited lower antimicrobial activity due to their inferior ion exchange capacity. These results are consistent with the silver content of the carriers.

Table 3. Minimal inhibition concentrations (MICs) of different antibacterial agents.

Antibacterial Agents	Ag-LTA	Ag-Y	Ag-M	Ag-V
MIC (µg/mL)	150	250	400	600

The results of the antibacterial ring inhibition tests for the four types of antibacterial agents are shown in Figure 4. Among the suspension test groups, the control group shows a minimal-absent inhibition ring, while the Ag-LTA, Ag-Y, and Ag-M antimicrobial agents exhibit significant antibacterial effects. The Ag-V antimicrobial agent displayed a weaker effect, suggesting a limited diffusion capability of its silver ions on solid culture media. Despite having a lower silver content, the Ag-M antimicrobial agent demonstrated comparable antibacterial activity to the zeolite antimicrobial agents, owing to its strong diffusion capacity. Zeolite antimicrobial agents, characterized by predominantly microporous channels, facilitate ion exchange rather than diffusion within the channels, making the diffusion of silver ions relatively facile. Moreover, the larger particle size of vermiculite results in fewer antibacterial particles being immersed during the preparation of the antimicrobial disk, thereby influencing its antibacterial efficacy in the disk experiment. The trend of antibacterial activity tested with pellets was similar to that in the suspension test, but the difference is not exactly the same. Vermiculite shows higher antimicrobial activity when eliminating the size effect on the particle loading amount in the suspension test. To investigate the antimicrobial activities of the carriers, zeolite LTA was used for comparison, and we can see from Figure 4b that the carrier material shows no antimicrobial ability. Similarly, none of the other carriers show any sterilization capacity (pictures not shown).

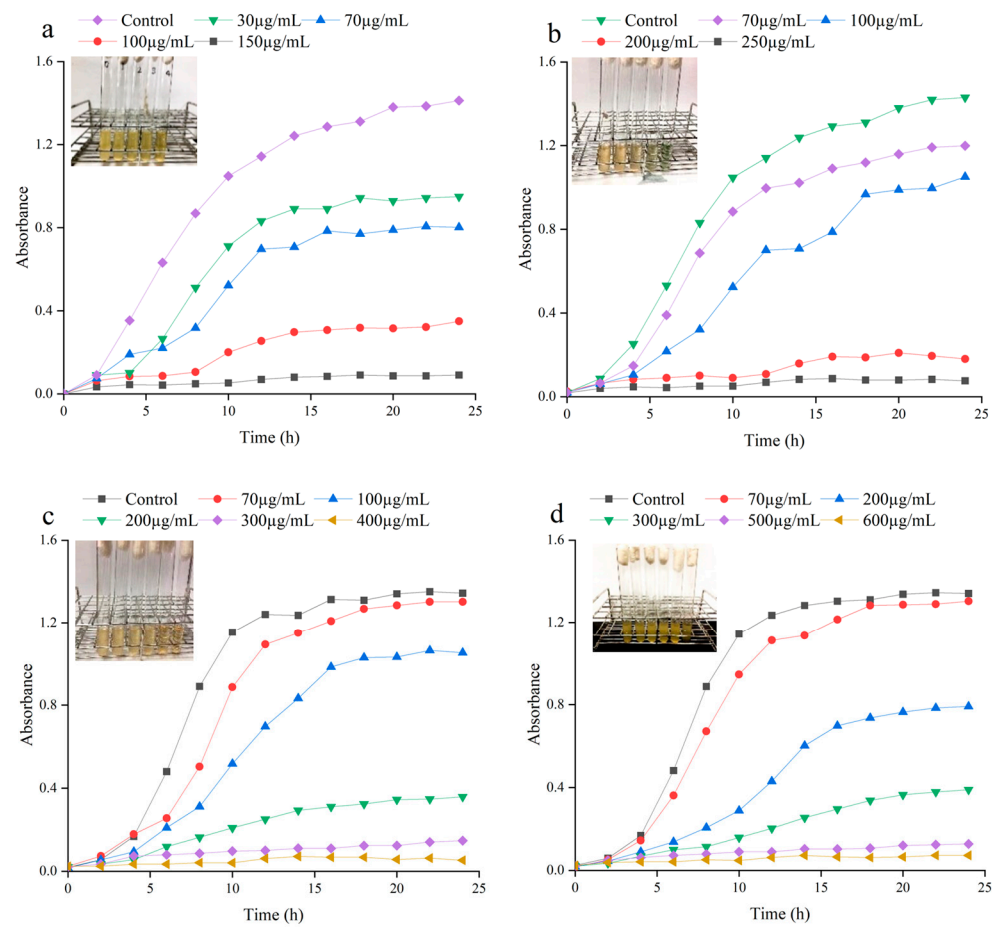


Figure 3. The growth of *E. coli* at different concentrations with four antimicrobial agents: (a) Ag-LTA; (b) Ag-Y; (c) Ag-M; (d) Ag-V. The insets show the pictures of the bacterial suspensions at different agent concentrations and the concentration increases from left to right.

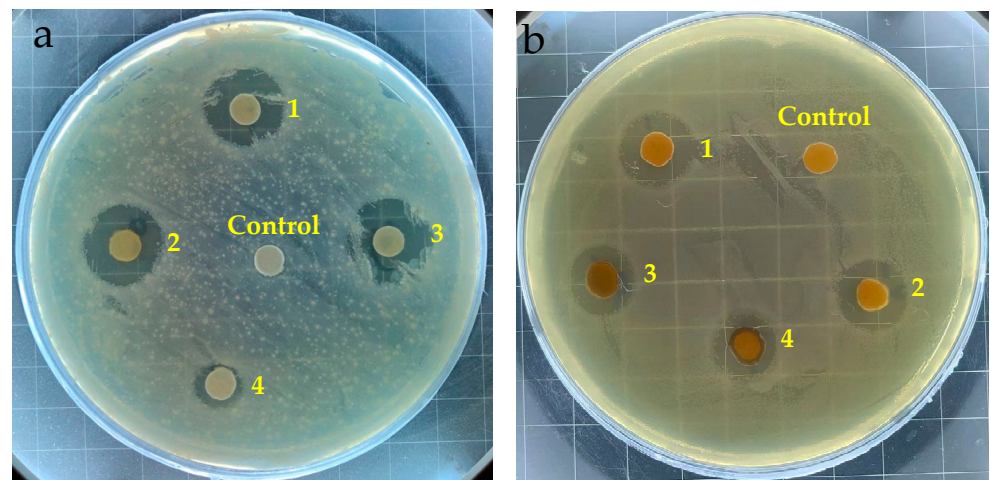


Figure 4. Experimental results of inhibitory halos. (a) Filter paper discs soaked in a suspension with/without antimicrobial agents. Control—without antimicrobial agents; 1—with Ag-LTA; 2—with Ag-Y; 3—with Ag-M; 4—with Ag-V. (b) Antimicrobial agent pellets. Control—pure LTA; 1—Ag-LTA; 2—Ag-Y; 3—Ag-M; 4—Ag-V.

3.3. Antibacterial Properties of Coatings

The MIC and antibacterial ring inhibition tests indicated the high activities of the antimicrobial agents. However, they cannot directly reflect the coating properties, since the agents are bound in the coating matrix instead of being in a free state, so the antimicrobial activity of coatings was evaluated. The continuous and controlled release of active silver ions from the coating surface to the pathogenic environment is a critical factor for the effectiveness of antimicrobial products. The antimicrobial efficacy relies on the concentration of silver ions, which, in turn, is primarily influenced by the ion strength of the medium. Figure 5 illustrates the antimicrobial properties of the coated plates under consistent medium-ion-strength conditions. The test solution containing a 0.85 wt% NaCl solution enables the sodium ions to serve as environmental ions that replace silver ions on the carriers through ion exchange, facilitating the release of silver ions into the surrounding environment. Most body fluids, e.g., sweat, contain sodium or other cations, so this test mimics real-world human contact with the coatings. In hospitals or other public areas, when sweaty hands or other body parts make contact with contaminated surfaces, the cations in the body fluid would activate the antimicrobial coatings. The thickness of all the coating films was maintained at 55–65 μm for consistency. To eliminate the possibility that the antimicrobial effect was a result of the carriers themselves, antimicrobial tests were also conducted on coatings with pure carrier agents. The results show no antimicrobial activity was present for any of the four carriers. In addition, all the antimicrobial tests on silver agents were conducted three times, and the standard deviation was within 1% for each agent (the error bars are too small to be seen for some data points), indicating consistent and stable activity.

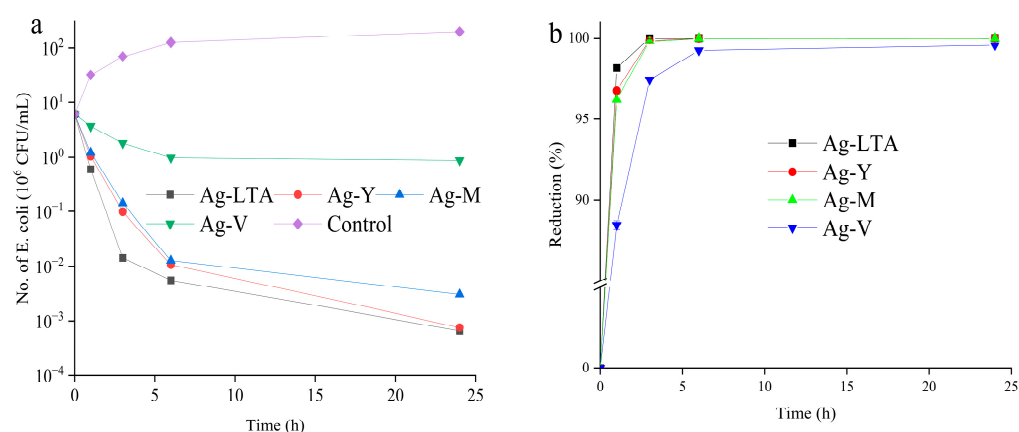


Figure 5. Antimicrobial properties of several antimicrobial coatings: (a) the variation of No. of *E. coli* with time on different antimicrobial coatings; (b) the reduction rate of *E. coli* with time on different antimicrobial coatings.

Compared with commercial agents, all the antibacterial agents present higher antibacterial activities with reduction rates of over 99% (Table 4). It can be seen in Figure S2 that the No. of *E. coli* is dramatically reduced after treatment with the antimicrobial coatings. Among the four agents, the Ag-LTA zeolite antimicrobial agent exhibited rapid bactericidal effects. Within the first 6 h, it showed the steepest decline in bacterial count, indicating strong antimicrobial efficacy within a short period. Moreover, the Ag-LTA coatings withstand seven washing cycles, indicating great durability (Figure 6). Comparatively, the antimicrobial activity of the Ag-Y antimicrobial agent is initially weaker than that of Ag-LTA, but the bacterial count reaches a similar level after 24 h, suggesting comparable long-term effectiveness. On the other hand, Ag-M antimicrobial plates exhibit similar initial antimicrobial effects to Ag-Y, but the bacterial count remains higher after 24 h, resulting in slightly inferior efficacy. Nonetheless, there is still a three-order-of-magnitude reduction in bacterial count, achieving a sterilization efficiency that exceeds 99.9%. In contrast, the Ag-V antimicrobial plates show relatively poor sterilization efficacy, with only

a one-order-of-magnitude decrease in bacterial count within 24 h; however, it still achieved a sterilization rate that exceeded 99 % compared to the control group. Zeolite antimicrobial agents, characterized by their large exchangeable ion capacity and abundance of silver ions, also have a high surface area, a small particle size, and a high water absorption capacity. These characteristics lead to uniform dispersion in coatings and an increased rate for the ion exchange process, resulting in higher silver ion release and improved antimicrobial performance. Similarly, clay-based antimicrobial agents also possess strong water absorption capacity, promoting the release of silver ions.

Table 4. Antimicrobial activity of surface coatings after exposure for 6 hrs.

Coating Samples	Log (<i>E. coli</i> No.)	% Reduction
Control	7.84	-
Zeomic® AJ10N/D	6.54	94.93%
Zeomic® AW 10N/D	6.77	91.44%
Microkiller® SRT-104	6.62	93.92%
Ag-LTA	2.82	>99.99%
Ag-Y	2.88	>99.99%
Ag-M	3.48	99.99%
Ag-V	5.94	99.21%

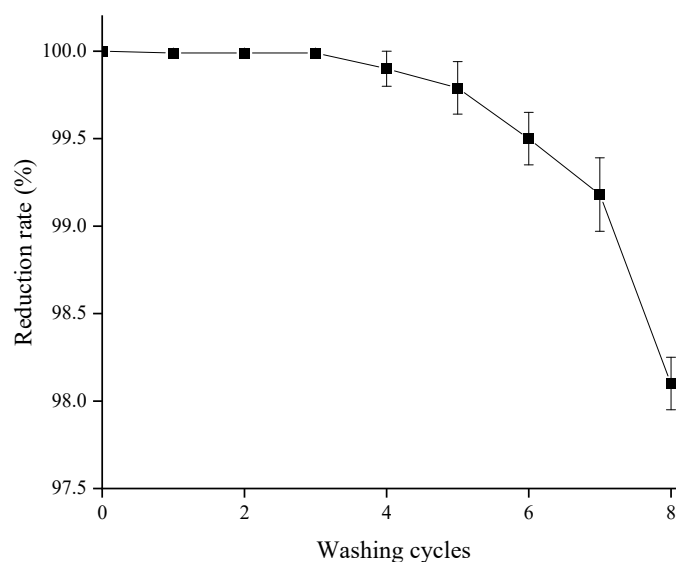


Figure 6. Antimicrobial durability of coatings with Ag-LTA agent after several washing cycles.

The leaching test of Ag^+ from antimicrobial coatings showed that the concentration of leaching Ag^+ in the solution is 0.026 mg/L, which is lower than the tolerance of releasing silver (under 0.1 mg/L) in drinking water that is recommended by the World Health Organization (WHO) and the US EPA. Therefore, the application of silver ions in this powder coating system has no safety issues.

3.4. Properties of the Antibacterial Coatings

The color of the coating surface is a crucial parameter that indicates the state of the silver within the coating. When silver ions undergo a reduction to nano silver, the coating color changes to yellow, which significantly impacts the overall appearance of the coating. The reduction of silver ions to metallic silver leads to a more significant yellowish color difference [31]. This is also verified by the XPS spectrum of the Ag 3d region (Figure S3) for the Ag-LTA agent. The peak positions of Ag 3d_{3/2} and Ag 3d_{5/2} were 374.0 and 367.8 eV, respectively. The peak center of Ag 3d_{5/2} is located between 368.2 eV (corresponding to Ag^0) and 367.4 eV (corresponding to Ag^+); this indicates the

coexistence of silver ions and elemental silver [23,32]. Ideally, it is desirable for the silver on the coating surface to exist in the form of ions, enabling it to promptly engage in combating microorganisms when necessary. Table 5 presents the color difference results of the four antimicrobial coatings compared to the control group without antimicrobial additives. The color difference parameters measured include ΔE , ΔL , Δb , and Δa . Figure 7 provides visual representations of the coatings containing the four antibacterial additives. Upon the addition of antimicrobial agents, the color of the coatings undergoes varying degrees of change. Notably, the Δb value indicates the most significant shift towards a yellow color. This can be attributed to the high reduction potential of silver ions, which makes them prone to reduction during the high-temperature curing process that is necessary for the coating. Consequently, fine silver particles are formed and adhere to the surface, imparting a distinct yellow hue to the coating.

Table 5. Color analysis and mechanical properties of coating surface containing four antimicrobial additives.

Parameter	Control	Ag-LTA	Ag-Y	Ag-M	Ag-V
L	-	-2.63	-2.68	-5.24	-4.36
a	-	-0.63	-0.89	-1.17	-0.59
b	-	8.32	11.08	11.24	10.59
E	-	8.74	11.43	12.45	11.46
Impact resistance	Pass ¹	Pass	Pass	Pass	Pass
Adhesive strength	Rate 0 ²	Rate 0	Rate 0	Rate 0	Rate 0
Pencil hardness	HB	HB	HB	HB	HB

¹: The coating can stand an impact of 490 N·cm. ²: No material of coating is peeled off.



Figure 7. The appearance of the coatings containing the four antimicrobial additives, from left to right: Ag-LTA, Ag-Y, Ag-M, and Ag-V.

Among the different carriers, the extent of yellowing caused by the Ag-LTA antimicrobial agent is the lowest. This can be attributed to the restricted formation of elemental silver within the confined interior space of the α -cage structure, providing protection to the silver ions. In contrast, montmorillonite and vermiculite carriers with larger internal spaces, such as mesoporous and macroporous spaces, exhibit more pronounced yellowing. Furthermore, clay-based carriers with larger pore sizes facilitate the detachment of silver ions from the carrier, leading to their reduction in response to the external environment.

The morphologies of antibacterial coatings are exhibited in Figure S4. Agents with silver ions can be clearly seen on the coating surface except the coating with Ag-V, which is with the lowest silver loading. The mechanical properties were characterized by impact resistance, hardness, and adhesive strength tests, as shown in Table 5. Compared to the control sample, the antimicrobial coatings with different agents present the same high

impact resistance, hardness, and adhesive strength. The introduction of agents does not damage the coating structure and properties.

4. Conclusions

In this paper, we investigated the antimicrobial properties and application of silver ion antimicrobial agents with different carriers in powder coatings. Each carrier has its unique characteristics, and their effect on antimicrobial efficacy varies due to differences in cation exchange capacity and pore size. Among them, the Ag-LTA zeolite antimicrobial agent demonstrates the highest effectiveness. The LTA zeolite not only has a high surface area, a small particle size, and a high silver content, but also provides a protection effect to silver ions, since the confined spaces within the sieve restrict the reduction of silver ions to some extent. The Y-type zeolite antimicrobial agent exhibits good antimicrobial performance. However, its high silicon–aluminum ratio and low cation exchange capacity result in lower silver loading efficiency. Additionally, the larger pore size of the Y-type zeolite makes the silver ions more susceptible to detachment from the carrier. In the presence of external environmental influences, they are more prone to reduction, leading to significant yellowing of the coating film. Antimicrobial agents utilizing clay-based carriers have even lower cation exchange capacity, resulting in poorer antimicrobial effectiveness. The Ag-V antimicrobial agent, for instance, achieves the lowest reduction rate after 24 h. The larger particle size of montmorillonite and vermiculite significantly impacts the appearance of the coating film, causing it to darken. Moreover, due to their larger pore size, silver ions readily detach from these carriers and undergo reduction reactions in the external environment. The degree of yellowing in the coating is consequently larger compared to the coatings with zeolite-type carriers. This paper studied the effect of zeolite- and clay-based carriers on the properties of Ag antimicrobial agents in the green powder coating system and provides guidance for the fabrication of active antimicrobial agents and coatings. It is noted that color changes for coating samples with different carrier materials are all relatively large; therefore, the questions of how to protect silver ions from reduction and how to maintain the high quality of the coatings are also worth studying. Additionally, strategies to improve the antimicrobial durability either through the control of silver release or recharging the coating with silver ions in some special application scenarios will be studied in future work.

Supplementary Materials: The following supporting information can be downloaded at: <https://www.mdpi.com/article/10.3390/coatings14030297/s1>, Figure S1: The process of preparation of antimicrobial coating film; Figure S2: The image of E. coli after treated with antibacterial coatings (diluted by 1000 times) a: coating without antibacterial agents; b: coating with Ag-LTA; c: coating with Ag-V; Figure S3: XPS spectrum the Ag 3d region of Ag-LTA; Figure S4 SEM images and EDS mapping (element Ag) of antimicrobial coatings with different agents: a, b, Ag-LTA; c, d, Ag-Y; e, f, Ag-M; g, h, Ag-V

Author Contributions: Conceptualization, H.Z. (Haiping Zhang), J.Z. and H.Z. (Hui Zhang); methodology, H.Z. (Haiping Zhang), J.C., X.Z. and Y.S.; validation, Y.S., J.C. and X.Z.; investigation, J.C., J.Y. and H.Y.; writing—original draft preparation, H.Z. (Haiping Zhang) and J.C.; writing—review and editing, H.Y., J.Y., H.Z. (Haiping Zhang) and H.Z. (Hui Zhang); supervision, J.Z., Y.S. and H.Z. (Hui Zhang); project administration, J.Z., Y.S. and H.Z. (Hui Zhang); funding acquisition, H.Z. (Haiping Zhang) and H.Z. (Hui Zhang). All authors have read and agreed to the published version of the manuscript.

Funding: The authors are grateful to the National Natural Science Foundation of China (Grant No. 22108198) and the Foshan Science and Technology Bureau (Foshan Science and Technology Innovation Project 1920001000150–08) for the financial support.

Institutional Review Board Statement: Not applicable.

Informed Consent Statement: Not applicable.

Data Availability Statement: The data presented in this study are available in the Supplementary Material.

Conflicts of Interest: The author Xinping Zhu was employed by the company Wesdon River Powder Paint Scientific Research Co., Ltd. The remaining authors declare that the research was conducted in the absence of any commercial or financial relationships that could be construed as a potential conflict of interest.

References

1. Dietz, L.; Horve, P.F.; Coil, D.A.; Fretz, M.; Eisen, J.A.; Van Den Wymelenberg, K. 2019 Novel Coronavirus (COVID-19) Pandemic: Built Environment Considerations to Reduce Transmission. *mSystems* **2020**, *5*, e00245-20. [[CrossRef](#)]
2. Tiwari, A. Handbook of Antimicrobial Coatings. In *Antimicrobial Coatings Technology Advancement or Scientific Myth*; Elsevier: Amsterdam, The Netherlands, 2018; pp. 5–25.
3. Spyrou, E. *Powder Coatings: Chemistry and Technology*; Vincentz Network GmbH & Co. KG: Hanover, Germany, 2012; pp. 71–77.
4. Czachor-Jadacka, D.; Pilch-Pitera, B. Progress in development of UV curable powder coatings. *Prog. Org. Coat.* **2021**, *158*, 106355. [[CrossRef](#)]
5. Kanwal, Z.; Raza, M.A.; Riaz, S.; Manzoor, S.; Tayyeb, A.; Sajid, I.; Naseem, S. Synthesis and characterization of silver nanoparticle-decorated cobalt nanocomposites (Co@AgNPs) and their density-dependent antibacterial activity. *R. Soc. Open Sci.* **2019**, *6*, 182135. [[CrossRef](#)] [[PubMed](#)]
6. Dutta, P.; Wang, B. Zeolite-supported silver as antimicrobial agents. *Coord. Chem. Rev.* **2019**, *383*, 1–29. [[CrossRef](#)]
7. Budama, L.; Çakır, B.A.; Topel, Ö.; Hoda, N. A new strategy for producing antibacterial textile surfaces using silver nanoparticles. *Chem. Eng. J.* **2013**, *228*, 489–495. [[CrossRef](#)]
8. Li, H.; You, Q.; Feng, X.; Zheng, C.; Zeng, X.; Xu, H. Effective treatment of Staphylococcus aureus infection with silver nanoparticles and silver ions. *J. Drug Deliv. Sci. Technol.* **2023**, *80*, 104165. [[CrossRef](#)]
9. Parvekar, P.; Palaskar, J.; Metgud, S.; Maria, R.; Dutta, S. The minimum inhibitory concentration (MIC) and minimum bactericidal concentration (MBC) of silver nanoparticles against Staphylococcus aureus. *Biomater. Investig. Dent.* **2020**, *7*, 105–109. [[CrossRef](#)]
10. Tsai, C.-H.; Whiteley, C.G.; Lee, D.-J. Interactions between HIV-1 protease, silver nanoparticles, and specific peptides. *J. Taiwan Inst. Chem. Eng.* **2019**, *103*, 20–32. [[CrossRef](#)]
11. Kumar, S.D.; Singaravelu, G.; Ajithkumar, S.; Murugan, K.; Nicoletti, M.; Benelli, G. Mangrove-Mediated Green Synthesis of Silver Nanoparticles with High HIV-1 Reverse Transcriptase Inhibitory Potential. *J. Clust. Sci.* **2017**, *28*, 359–367. [[CrossRef](#)]
12. Luis Cerrillo, J.; Eduardo Palomares, A.; Rey, F.; Valencia, S.; Bernardita Perez-Gago, M.; Villamon, D.; Palou, L. Functional Ag-Exchanged Zeolites as Biocide Agents. *Chemistryselect* **2018**, *3*, 4676–4682. [[CrossRef](#)]
13. Zhang, H.; Cui, J.; Zhu, J.; Shao, Y.; Zhang, H. Fabrication of Nano-Silver-Silver Ion Composite Antibacterial Agents for Green Powder Coatings. *Coatings* **2023**, *13*, 575. [[CrossRef](#)]
14. Hossain, S.I.; Kukushkina, E.A.; Izzi, M.; Sportelli, M.C.; Picca, R.A.; Ditaranto, N.; Cioffi, N. A Review on Montmorillonite-Based Nanoantimicrobials: State of the Art. *Nanomaterials* **2023**, *13*, 848. [[CrossRef](#)]
15. Vlad-Bubulac, T.; Hamciuc, C.; Serbezeanu, D.; Suflet, D.M.; Rusu, D.; Lisa, G.; Anghel, I.; Preda, D.-M.; Todorova, T.; Rimbu, C.M. Organophosphorus Reinforced Poly(vinyl alcohol) Nanocomposites Doped with Silver-Loaded Zeolite L Nanoparticles as Sustainable Materials for Packaging Applications. *Polymers* **2023**, *15*, 2573. [[CrossRef](#)]
16. Saint-Cricq, P.; Kamimura, Y.; Itabashi, K.; Sugawara-Narutaki, A.; Shimojima, A.; Okubo, T. Antibacterial Activity of Silver-Loaded “Green Zeolites”. *Eur. J. Inorg. Chem.* **2012**, *2012*, 3398–3402. [[CrossRef](#)]
17. Asraf, M.H.; Sani, N.S.; Williams, C.D.; Jemon, K.; Malek, N.A.N.N. In situ biosynthesized silver nanoparticle-incorporated synthesized zeolite A using Orthosiphon aristatus extract for in vitro antibacterial wound healing. *Particuology* **2022**, *67*, 27–34. [[CrossRef](#)]
18. Torkian, N.; Bahrami, A.; Hosseini-Abari, A.; Momeni, M.M.; Abdolkarimi-Mahabadi, M.; Bayat, A.; Hajipour, P.; Amini Rourani, H.; Abbasi, M.S.; Torkian, S.; et al. Synthesis and characterization of Ag-ion-exchanged zeolite/TiO(2) nanocomposites for antibacterial applications and photocatalytic degradation of antibiotics. *Environ. Res* **2022**, *207*, 112157. [[CrossRef](#)]
19. Roy, A.; Butola, B.S.; Joshi, M. Synthesis, characterization and antibacterial properties of novel nano-silver loaded acid activated montmorillonite. *Appl. Clay Sci.* **2017**, *146*, 278–285. [[CrossRef](#)]
20. Phongphut, A.; Chayasombat, B.; Cass, A.E.G.; Sirisuk, A.; Phisalaphong, M.; Prichanont, S.; Thanachayanont, C. Clay/au nanoparticle composites as acetylcholinesterase carriers and modified-electrode materials: A comparative study. *Appl. Clay Sci.* **2020**, *194*, 105704. [[CrossRef](#)]
21. Wang, Q.; Wang, M.; Lei, C.; Yan, L.; Wu, X.; Li, L. Functionalizing graphene with clay nanosheets as a protein carrier. *Colloid Interface Sci. Commun.* **2022**, *48*, 100618. [[CrossRef](#)]
22. Drelich, J.; Li, B.; Bowen, P.; Hwang, J.-Y.; Mills, O.; Hoffman, D. Vermiculite decorated with copper nanoparticles: Novel antibacterial hybrid material. *Appl. Surf. Sci.* **2011**, *257*, 9435–9443. [[CrossRef](#)]
23. Sun, Z.; Fan, C.; Tang, X.; Zhao, J.; Song, Y.; Shao, Z.; Xu, L. Characterization and antibacterial properties of porous fibers containing silver ions. *Appl. Surf. Sci.* **2016**, *387*, 828–838. [[CrossRef](#)]
24. Malachova, K.; Praus, P.; Rybkova, Z.; Kozak, O. Antibacterial and antifungal activities of silver, copper and zinc montmorillonites. *Appl. Clay Sci.* **2011**, *53*, 642–645. [[CrossRef](#)]
25. Cui, J.; Shao, Y.; Zhang, H.; Zhang, H.; Zhu, J. Development of a novel silver ions-nanosilver complementary composite as antimicrobial additive for powder coating. *Chem. Eng. J.* **2021**, *420*, 127633. [[CrossRef](#)] [[PubMed](#)]

26. Kitsopoulos, K.P. Cation-Exchange Capacity (CEC) of Zeolitic Volcaniclastic Materials: Applicability of the Ammonium Acetate Saturation (AMAS) Method. *Clays Clay Miner.* **1999**, *47*, 688–696. [[CrossRef](#)]
27. GB/T 1732-2020; Determination of Impact Resistance of Coating Films. National Standardization Administration: Beijing, China, 2020.
28. ASTM D3363-05-2011; Standard Test Method for Film Hardness by Pencil Test. ASTM International: West Conshohocken, PA, USA, 2011.
29. GB/T 9286-1998; Paints and Varnishes--Cross Cut Test for Films. National Standardization Administration: Beijing, China, 1998.
30. ASTM 2180-07; Standard Test Method for Determining the Activity of Incorporated Antimicrobial Agent(s) In Polymeric or Hydrophobic Materials. ASTM International: West Conshohocken, PA, USA, 2012.
31. Cui, J.; Yeasmin, R.; Shao, Y.; Zhang, H.; Zhang, H.; Zhu, J. Fabrication of Ag⁺, Cu²⁺, and Zn²⁺ Ternary Ion-Exchanged Zeolite as an Antimicrobial Agent in Powder Coating. *Ind. Eng. Chem. Res.* **2020**, *59*, 751–762. [[CrossRef](#)]
32. Lai, Y.; Chen, Y.; Zhuang, H.; Lin, C. A facile method for synthesis of Ag/TiO₂ nanostructures. *Mater. Lett.* **2008**, *62*, 3688–3690. [[CrossRef](#)]

Disclaimer/Publisher’s Note: The statements, opinions and data contained in all publications are solely those of the individual author(s) and contributor(s) and not of MDPI and/or the editor(s). MDPI and/or the editor(s) disclaim responsibility for any injury to people or property resulting from any ideas, methods, instructions or products referred to in the content.